Climatology of Flood-Producing Storms and Their Associated Rainfall Characteristics in the United States

Erin Dougherty[1*] and Kristen L. Rasmussen[*]

[*]*Department of Atmospheric Science*
Colorado State University
Fort Collins, CO

Submitted to Monthly Weather Review
January 2019
Revised May and July 2019

[1] *Corresponding Author*: Erin Dougherty, Department of Atmospheric Science, Colorado State University, Fort Collins, CO
Email address: edough@rams.colostate.edu
Phone number: (970) 491-8682
Fax number: (970) 491-8449

Early Online Release: This preliminary version has been accepted for publication in *Monthly Weather Review*, may be fully cited, and has been assigned DOI 10.1175/MWR-D-19-0020.1. The final typeset copyedited article will replace the EOR at the above DOI when it is published.

Abstract

Floods are one of the deadliest weather-related natural disasters in the continental United States (CONUS). Given that rainfall intensity and the amount of CONUS population exposed to floods is expected to increase in the future, it is critical to understand flood characteristics across the CONUS. Therefore, the purpose of this study is to develop a flood-producing storm climatology over the CONUS from 2002–2013 to better understand rainfall characteristics of these storms and spatiotemporal differences across the country. Flood reports from the NCEI Storm Events Database are grouped by causative meteorological event and are merged with the Shen et al. (2017) database of stream gauge-indicated floods to provide a robust indication of significant hydrologic events with a meteorological linkage. High-resolution Stage IV rainfall data was matched to 5559 flood episodes across the CONUS to identify rainfall characteristics of flood-producing storms in a variety of environments. This storm climatology indicates that flash flood-producing storms frequently occur with high rainfall accumulations in the summer east of the Rockies. Slow-rise flood-producing storms frequently occur in the spring–early summer (winter), with high rainfall accumulations over the northern and central CONUS (Pacific Northwest) due to rain-on-snowmelt, synoptic systems, and mesoscale convective systems (atmospheric rivers). Hybrid flood-producing storms, sharing characteristics of flash and slow-rise floods, frequently occur in spring–summer and have high rainfall accumulations in the central CONUS, Northeast, and Mid-Atlantic. Results from this climatology may provide useful for emergency managers, city planners, and policy makers seeking efforts to protect their communities against risks associated with flood-producing storms.

Accepted for publication in *Monthly Weather Review*. DOI 10.1175/MWR-D-19-0020.1.

1. Introduction

Floods are a major hazard across the world and are one of the deadliest weather-related natural disasters in the continental United States (CONUS; Ashley and Ashley 2008b). Well-known floods such as the Rapid City, South Dakota flood of 1972 and Big Thompson flood of 1976 resulted in 220 and 144 fatalities, respectively (Maddox et al. 1978). The more recent Colorado flood of 2013, which was a result of 450 mm of rain that fell in a week over the Front Range of Colorado, led to 8 fatalities and over $2 million in damage (Gochis et al. 2015). Flooding from Hurricane Harvey (2017) in the Houston, Texas area resulted in record rainfall (1548.7 mm) from a tropical cyclone in the CONUS and is the second costliest storm in U.S. history ($125 billion in damage; NHC 2018). These examples illustrate that despite occurring in different locations and due to different causes, floods in the CONUS result in tremendous amounts of damage.

Estimates of flood exposure over the past several decades show an increasing trend in urban areas such as Atlanta, Georgia (Ferguson and Ashley 2017); New York City, New York; and Miami, Florida (Qiang et al. 2017), despite a decreasing trend nationwide (Qiang et al. 2017). Though estimates of current nationwide flood exposure might not agree, studies show that *future* flood exposure (Wing et al. 2018) and disaster probability (Freeman and Ashley 2017) will increase over the CONUS under various growth scenarios. Additionally, given the projected increased intensity of extreme precipitation over the CONUS in a future climate (Allen and Ingram 2002; IPCC 2013; Prein et al. 2017), it is suggested that the U.S. population is becoming increasingly vulnerable to flood-associated risks. Thus, it is critical to better understand the characteristics of floods across the CONUS in order to identify which regions are most

Accepted for publication in *Monthly Weather Review*. DOI 10.1175/MWR-D-19-0020.1.

71 vulnerable to floods in a current climate, so that these risks can be better estimated in the future
72 climate.

73 The cause of floods involves complex hydrologic, geomorphologic, and atmospheric
74 interactions, and is defined by the National Weather Service (NWS) as "the inundation of
75 normally dry area caused by an increased water level in an established watercourse, or ponding
76 of water, that poses a threat to life and property" (NWS 2007). This definition can include flash
77 floods, slow-rise floods, and coastal floods, amongst others. Though predicting floods is
78 complicated, NWS forecasters rely on key atmospheric variables to indicate where anomalous
79 precipitation is probable to issue flood watches and warnings (Schroeder et al. 2016a). Similar
80 conditions between high-impact floods, like the Big Thompson (1976) and Rapid City (1972)
81 floods, both of which involved orographic lift of unstable and anomalously moist air up the edge
82 of high terrain (Maddox et al. 1978), suggested that certain atmospheric "ingredients" are
83 necessary to produce floods. However, prior studies primarily relied on pattern recognition of
84 synoptic and mesoscale conditions to understand factors leading to flooding (Maddox et al. 1979;
85 Funk 1991), rather than a more comprehensive view of numerous ingredients that could cause
86 floods (Doswell et al. 1996). These ingredients were explicitly outlined in the Doswell et al.
87 (1996) "ingredients-based approach" for flash flood forecasting, which emphasized that for
88 floods to occur, multiple ingredients are necessary. Ingredients leading to high rainfall
89 accumulation include high rainfall rates and long duration, as given by the following equation:

90 $$P = \bar{R}D \qquad \text{Eqn. 1}$$

91 where P is the rainfall accumulation, $\bar{R}$ is the average rainfall rate, and D is the rainfall duration
92 (Doswell et al. 1996). High rain rates are due to factors that enhance precipitation efficiency,
93 including ample moisture and a lifting mechanism, while long-duration rainfall can be caused by

Accepted for publication in *Monthly Weather Review*. DOI 10.1175/MWR-D-19-0020.1.

quasi-stationary convective and/or synoptic systems (Doswell et al. 1996). These ingredients, particularly anomalously high precipitable water, were present in the Big Thompson and Rapid City floods (Maddox et al. 1978; Caracena et al. 1979), as well as a majority of urban flash floods over the CONUS (Schroeder et al. 2016b).

Case studies of floods around the world have additionally exemplified the importance of how the Doswell et al. (1996) ingredients manifest in different ways. A flash flood in Leh, India in August 2010 was the result of upslope flow of moist, conditionally unstable air along a steep edge of the Himalayas and anomalous quasi-stationary synoptic conditions over the Tibetan plateau with an associated easterly low-level jet that combined to form a series of mesoscale convective systems (MCSs) propagating over the Himalayas (Rasmussen and Houze 2012). In Pakistan, long-lived flooding from July–August 2010 was due to a quasi-stationary synoptic pattern and channeling of anomalous moisture into the region towards the Himalayan barrier that caused prolonged stratiform precipitation (Houze et al. 2011). The Colorado flood of 2013 and Uttarakhand, India floods in June 2013 similarly involved upslope flow of moist air over a prolonged period of time (several days to weeks), but these floods were characterized by stratiform rainfall with embedded weak to moderate convection, unlike the previous U.S. flash flood cases (Gochis et al. 2015; Houze et al. 2017). Therefore, similar "ingredients" defined by Doswell et al. (1996) are responsible for a variety of flood types around the world.

From a climatological perspective, heavy rainfall has been utilized as a proxy for flooding in the CONUS, as suggested by Doswell et al. (1996). Maddox et al. (1979) utilized National Oceanic and Atmospheric Administration (NOAA) storm data to examine atmospheric regimes associated with flash floods, highlighting the importance of fronts, synoptic systems, and thunderstorm outflow boundaries for triggering intense rainfall. Brooks and Stensrud (2000),

Accepted for publication in *Monthly Weather Review*. DOI 10.1175/MWR-D-19-0020.1.

Schumacher and Johnson (2006), Kunkel et al. (2012), and Stevenson and Schumacher (2014) developed climatologies of heavy rain events over the CONUS using data from rain gauges and Stage IV precipitation data. These studies found that heavy rainfall peaked in the summer (Maddox et al. 1979; Brooks and Stensrud 2000; Schumacher and Johnson 2006; Stevenson and Schumacher 2014), and were due to mesoscale convective systems (MCSs) in the Central U.S. (Schumacher and Johnson 2006; Kunkel et al. 2012), the monsoon in the Southwest (Kunkel et al. 2012), extratropical cyclones in the Pacific Northwest (Kunkel et al. 2012), and tropical cyclones in the eastern U.S. (Schumacher and Johnson 2006; Kunkel et al. 2012). Though these heavy rainfall climatologies provide a sense of probable flood occurrence over the CONUS, precipitation is not the only contributor to floods, with soil moisture storage capacity also being an important factor (Berghuijs et al. 2016), in addition to underlying geomorphology and hydrologic processes.

Given the complexity and risk of flooding in the CONUS (Ashley and Ashley 2008b), various CONUS-wide flood databases and climatologies have been developed that include numerous parameters, in addition to precipitation. Examination of factors in conjunction with precipitation is necessary to gain a comprehensive understanding of floods, since floods are caused by rain interacting with varying terrain gradients, soil types, vegetation, land use, and antecedent soil moisture conditions (Davis 2001). Gourley et al. (2013) created the Flooded Locations and Simulated Hydrographs (FLASH) database that combines United States Geologic Service (USGS) streamflow observations, NWS storm reports, and two-years' worth of survey responses that documents flash floods. Shen et al. (2017) also created a comprehensive database of over 0.5 million floods over the CONUS from 2002–2013 using USGS streamflow measurements to identify floods and Stage IV rainfall to provide contributing rainfall

Accepted for publication in *Monthly Weather Review*. DOI 10.1175/MWR-D-19-0020.1.

information. A number of studies have utilized these databases, especially the FLASH database. Saharia et al. (2017a) used the FLASH database (Gourley et al. 2013) to identify flash flood hotspots based on discharge peaks in the CONUS and to characterize floods more broadly in the CONUS based on season, climatic region, and basin geomorphology (Saharia et al. 2017b). Michaud et al. (2001) and Smith and Smith (2015) also used discharge to identify flash floods in the CONUS, based on discharge peaks in small-basins (10–200 km^2) and unit discharge exceeding 1 $m^3\ s^{-1}\ km^{-2}$, respectively. Ashley and Ashley (2008a) used the National Centers for Environment Information (NCEI; formerly National Climatic Data Center) Storm Report Data to identify deadly floods in the CONUS from 1996–2005 and their associated synoptic and mesoscale environments. Despite different flood identification metrics, these studies (and others) identify similar regional flood patterns over the CONUS: floods in the East have high discharge and precipitation, mainly associated with warm-season convective rainfall (Michaud et al. 2001; Smith and Smith 2015; Saharia et al. 2017a) or hurricanes (Ashley and Ashley 2008a); Western floods occur in steeper sloped basins in the winter for the West Coast (Smith and Smith 2015; Villarini et al. 2016) due to extratropical cyclones (Ashley and Ashley 2008a; Saharia et al. 2017a) and summertime in the Southwest (Michaud et al. 2001; Villarini et al. 2016) due to the monsoon (Ashley and Ashley 2008a; Saharia et al. 2017b).

While previous flood and heavy rainfall climatologies over the CONUS document various aspects of flooding (streamflow, extreme rain rates, fatalities), an important perspective related to the meteorological characteristics associated with specific floods is missing in the literature. Thus, the primary goal of the current study is to produce a climatology of rainfall characteristics in *flood-producing storms* in the CONUS. While flood databases like Shen et al. (2017) provide a thorough documentation of floods in the CONUS, the focus is more on

Accepted for publication in *Monthly Weather Review*. DOI 10.1175/MWR-D-19-0020.1.

hydrologic processes, as one flood event in their database could have multiple peaks in streamflow over a period spanning months (Mei and Anagnostou 2015), likely involving numerous meteorological systems. Other databases, like the comprehensive FLASH database (Gourley et al. 2013), only consider flash floods, and this study seeks to examine different flood types. The heavy rainfall climatologies are helpful from a forecasting-perspective, but do not translate directly to floods due to factors in addition to rainfall, such as terrain gradients, soil moisture, storm characteristics, and land use, needed for a flood to occur. Thus, this study fills a gap by examining the rainfall characteristics associated with flood-producing storms using the NCEI Storm Events Database, which identifies where flooding (as defined by the NWS) actually occurred and groups these floods by the associated meteorological system. The NCEI database integrated with the Shen et al. (2017) gauge-identified floods and Stage IV precipitation data provides a method of identifying floods from flood reports and stream gauges, and analyzing their associated rainfall characteristics over the CONUS from 2002–2013. Though the focus of this study is on the rainfall characteristics of floods, it is acknowledged that hydrologic, topographic, and land-use factors are vital for producing floods, and were inherent in generating the floods used in this database. Examination of these non-atmospheric factors is beyond the scope of the study, although their effects may be implicitly included in the methodology by matching precipitation associated with flood reports with peaks in streamflow consistent with river flooding. Note that throughout the manuscript, "floods" and "flood-producing storms" is used interchangeably.

The understanding gained from this climatology of the duration, rainfall accumulation, seasonality, and spatial occurrence associated with flood-producing storms is vital to increase awareness of rainfall-associated flood risks specific to individual regions. Additionally, this

Accepted for publication in *Monthly Weather Review*. DOI 10.1175/MWR-D-19-0020.1.

study provides a necessary first step in understanding the overall climatology of flood-producing storms over the CONUS to enable future research investigating how flood-producing storms may change in a future climate using high-resolution, convection-permitting simulations from Liu et al. (2016). Results from this climatology in conjunction with future research on flood-producing storms in a future climate will provide insights on current and future flood risk.

2. Data and Methods

a. NCEI Storm Events Database

The NCEI Storm Events Database is a documentation of notable meteorological events from January 1950–September 2017, available from the NCEI website[2]. NCEI receives details on the location, date, and time of these events primarily from NWS, as well as other outside sources, including media and law-enforcement. The events in the database include blizzards, hurricanes, hail, and floods, among a long list of others, and this study utilizes flood reports from 2002–2013. NCEI makes a distinction between flash floods and floods in the database. According to guidelines provided by NWS (NWS 2007), flash floods are defined by "a rapid and extreme flow of high water into a normally dry area, or rapid water level rise in a stream or creek above a predetermined flood level, beginning *within* six hours of the causative event (e.g., intense rainfall, dam failure, ice jam-related)," while floods are defined by "the inundation of a normally dry area caused by an increased water level in an established watercourse, or ponding of water, generally occurring *more* than six hours after the causative event, and posing a threat to life or property". For this reason, floods will be called slow-rise floods from this point forward, due to their longer temporal nature.

[2] https://www.ncdc.noaa.gov/stormevents/

Accepted for publication in *Monthly Weather Review*. DOI 10.1175/MWR-D-19-0020.1.

Note that the above NWS flood definitions are used primarily as a forecasting tool, thus, the flood classification in this study is not confined to the specific definition (or duration) given that a single flood episode can be composed of numerous storm reports (or events) and can be a mix of flash and slow-rise floods. This fact necessitated the creation of a separate category of floods–hybrid floods–when reports (or events) within the same episode were labeled as both flash and slow-rise floods. Though a single hybrid flood episode might be more or less flash or slow-rise in nature, having characteristics of both at any point makes these floods uniquely different in character and merits its own category, due to unique storm characteristics. An example of such a hybrid flood is the Colorado flood of 2013 (Gochis et al. 2015), which was a high-impact flood along the Front Range of Colorado that was both long-duration (nearly a week long), with "flashier" bouts of intense convection within stratiform rainfall, thus reported as both a flash and slow-rise flood.

Due to the somewhat subjective nature of these flood reports, there are limitations in using the NCEI Storm Events Database. Inaccuracies of these reports are acknowledged by NCEI, particularly when derived from sources beyond NWS. Other sources of error in this database include population biases and differences in reporting by NWS Weather Forecast Offices (WFOs). When examining the same dataset, Ashely and Ashley (2008b) found that eastern CONUS displayed more flood fatalities than the western CONUS, which they partially attributed to higher population in the East. It is an often-cited limitation of the Storm Events Database that report biases occur due to differences in population density by region, urban vs. rural areas, and at night (Barthold et al. 2015; Herman and Schumacher 2018). Additionally, the issuance of warnings and report encoding is known to differ by NWS WFOs, with some WFOs

Accepted for publication in *Monthly Weather Review*. DOI 10.1175/MWR-D-19-0020.1.

preferring to encode an event as flash flood rather than a flood (Neilsen et al. 2015; Herman and Schumacher 2018).

Despite the limitations of the Storm Events Database, this database is advantageous for the purposes of our study–to understand rainfall characteristics in flood-producing storms. First, the NCEI Storm Events Database contains a large sample of floods over the CONUS, with over 35,000 flood reports from 2002–2013 (Table 1). Secondly, Herman and Schumacher (2018), who studied flash flood verification over the CONUS, state that these flood reports, while underreported, likely have few false alarms. This provides confidence that the large sample of flood reports in the NCEI database capture actual flood occurrence, as opposed to peaks in streamflow or rainfall, which may or may not result in a flood. Finally, the database provides a meteorological-centric viewpoint of floods through the grouping of numerous flood reports (or "events") in a given location with a single flood episode, based on being associated with the same meteorological system (as defined by NWS; see NWS 2007). This is critical to the goal of the present study in taking a storm-centric viewpoint of the rainfall associated with floods (similar to Ashely and Ashley 2008a, though they examined flood fatalities), and is major reason for using this database over others. The flash, slow-rise, and hybrid floods from the NCEI database were examined over their entire storm lifecycle, and were matched to the Shen et al. (2017) database to associate flood reports to streamflow-identified floods.

b. Merging storm reports with the Shen et al. (2017) database

Shen et al. (2017) developed a comprehensive flood database over the CONUS from 2002–2013 using a characteristic point method (CPM) described by Mei and Anagnostou (2015). The CPM is an automated method used to identify flood events by the rising and recessing branches of a hydrograph using instantaneous United States Geological Services (USGS)

Accepted for publication in *Monthly Weather Review*. DOI 10.1175/MWR-D-19-0020.1.

streamflow values. Only peak streamflow values between the rising and recessing branches of the hydrograph that exceed the 80th percentile are utilized. Shen et al. (2017) additionally used basin-averaged Stage IV precipitation to associate the peak in streamflow with flood-triggering precipitation.

While the Shen et al. (2017) flood database is thorough and comprehensive, it does not meet the goals of the present study to focus on the rainfall input to floods from a storm-perspective. This was evident when examining the Shen et al. (2017) database (available at http://ucwater.engr.uconn.edu/fedb) that contained a nearly two-year long flood from August 2007–June 2009 in Wisconsin, with precipitation averaged over a two-year period. Clearly, no single storm or rain-producing system lasts for two years, with typical lifespans of rain-producing systems on the order of hours (thunderstorms), days (mesoscale convective systems), to weeks (hurricanes and extratropical cyclones). Thus, while the Shen et al. (2017) database is useful in identifying peaks in streamflow, including multiple closely-spaced peaks (Mei and Anagnostou 2015) that explain the two-year long flood in their database, it does not fit the precise needs of the present study.

However, to provide confidence that the NCEI Storm Reports used to identify floods in this study had a streamflow response, NCEI Storm Reports beyond three days and 200 km of gauge-identified floods by Shen et al. (2017) were excluded. A three-day period was chosen to account for a lag between start times in the Shen et al. (2017) database (based on the rising branch of the hydrograph) and the NCEI database (when the flood was reported, i.e., due to a rise in streamflow above a predetermined flood level or flow of water onto normally dry land; NWS 2007). A buffer of 200 km was selected based on average distances across various river basins, including the South Platte (Colorado), Wabash (Indiana), and Willamette (Washington) basins,

Accepted for publication in *Monthly Weather Review*. DOI 10.1175/MWR-D-19-0020.1.

providing confidence that the flood indicated by the Shen et al. (2017) database and the storm reports were in the same river basin, and thus, most likely associated with the same event. Matching the NCEI Storm Reports with floods from Shen et al. (2017) resulted in 15,932 (2,808) flash flood events (episodes), 10,614 (1,638) slow rise flood events (episodes), and 11,120 (1,113) hybrid flood events (episodes; Table 1). Among the hybrid floods, 6,786 (61%) of events were labeled as flash floods and 4,334 (39%) were labeled as slow-rise floods, giving a slight bias towards flash floods in this category.

c. Stage IV precipitation data

The lack of rainfall information in the storm report data was mitigated by the use of Stage IV precipitation data (Nelson et al. 2016). This data is available at a 4-km hourly resolution since 2001, and is a multi-sensor (radar-estimated rainfall combined with rain gauge data) precipitation analysis (MPE) produced by twelve River Forecast Centers (RFCs) over the CONUS. Regional MPEs are quality controlled by RFCs and merged into a national product by The National Centers for Environmental Prediction (NCEP; Lin and Mitchell 2005). Though errors exist in Stage IV data–discontinuities across RFC boundaries, sparser coverage over the Western CONUS due to less radar coverage and rain gauges, and quality control issues at the hourly timescale–Stage IV data is considered the benchmark precipitation estimate over the CONUS used to validate other precipitation data and high-resolution simulations (Nelson et. al 2016; Prein et al. 2017b; Rasmussen et al. 2017; Beck et al. 2019). This high-resolution, MPE dataset is necessary for studying rainfall associated with floods, as flood-producing rainfall can be transient and small-scale, especially in flash floods (Davis 2001). Despite these deficiencies, spatial patterns of flash flood rainfall characteristics in Stage IV hourly data compare quite well

Accepted for publication in *Monthly Weather Review*. DOI 10.1175/MWR-D-19-0020.1.

297 to TRMM 3B42 rainfall, providing confidence that physical rainfall characteristics are captured,
298 and not just artifacts of these errors.

299 In order to gather Stage IV data associated with floods identified from the Storm Events
300 Database (Section 2a), the location and duration of the reported flood episode was utilized. The
301 centroid of each flood episode was calculated based on geographic information obtained from
302 merging the storm reports with county shapefiles[3]. Hourly (every 3rd hourly) Stage IV rainfall
303 data were obtained over a radius of +/- 5° from the episode centroid for flash and hybrid (slow-
304 rise) floods, in order to capture the entire storm system's contribution to the reported flood. A
305 sensitivity test was conducted for varying radii, and at smaller radii, the flood-contributing
306 rainfall was cut-off, hence the use of the +/-5° radius. It is possible that even at this large of a
307 domain, some rainfall could be missed, due to flood waves propagating downstream from the
308 causative event. Every third hourly Stage IV rainfall file for slow-rise floods was utilized rather
309 than every hourly file due to the long-duration of these floods that resulted in an unmanageable
310 amount of data at the hourly scale. Note that when hourly Stage IV files were not available (i.e.,
311 for the Pacific Northwest RFC; Nelson et al. 2016), six hourly files were used instead, which
312 constituted 60 slow-rise flood episodes. These Stage IV files were analyzed for the duration of
313 each episode, which was provided in the storm report database, plus a buffer +/- 1 (6) hours for
314 flash (slow-rise and hybrid) floods to take into account possible rainfall occurrence before and/or
315 after the start of the reported flood event. The temporal buffers were chosen based on the
316 observation that flash floods are generally more transient, due to their convective nature (Davis
317 2001).

[3] https://www.census.gov/geo/maps-data/data/cbf/cbf_counties.html

Accepted for publication in *Monthly Weather Review*. DOI 10.1175/MWR-D-19-0020.1.

Given the large domains over which rainfall data was analyzed, the flood-contributing rainfall likely associated with each flood was isolated through an object-identifier tool in Python. This tool identified the largest contiguous precipitation area where the flood domain precipitation accumulation met or exceeded the 75th percentile. This method locates and isolates the maximum precipitation accumulation and the surrounding high accumulation for all floods, irrespective of the size of the precipitation swath–this allows for isolated convective rainfall to be captured, as well as larger-scale synoptic rainfall from MCSs, fronts, or extratropical cyclones. Such an example of this method isolating the heavy flash flood rainfall from lighter non-flash flood rainfall is shown in Fig. 1, and similarly isolates the maximum rainfall in slow-rise (not-shown), and hybrid floods (not-shown).

Various rainfall metrics were calculated for each flood episode, including accumulated rainfall, area, and duration of the largest contiguous rainfall area exceeding the 75th percentile of accumulation. These quantities were then averaged over the 12-year period for 1) each Stage IV 4-km grid cell and 2) all episodes by flood type. The number of floods per grid cell were also summed over the entire 12-year period to find the episode frequency. This calculation allowed for variables to be multiplied by a scaling factor similar to Rasmussen et al. (2016):

$$F = \frac{N_f}{N_T} \qquad \text{Eqn. 2}$$

where F is the scaling factor, N_f is the number of flood episodes per Stage IV grid cell, and N_t is the total number of flood episodes over the CONUS. These normalized variables allowed for a spatial comparison of flood characteristics over the CONUS, despite different episode frequencies.

3. Results

a. Seasonal and geographical distribution of floods

Accepted for publication in *Monthly Weather Review*. DOI 10.1175/MWR-D-19-0020.1.

341 The number of flood episodes per month is shown in Fig. 2, which has similarly been
342 shown in previous studies, though only for flash floods (Maddox et al. 1979; Brooks and
343 Stensrud 2000; Schumacher and Johnson 2006). Flash floods display a warm-season maximum
344 from May to August. An absolute maximum occurs in July, which is consistent with findings of
345 heavy rainfall seasonality from Maddox et al. (1979), Brooks and Stensrud (2000), Schumacher
346 and Johnson (2006), and Stevenson and Schumacher (2014). A spring to early summer
347 maximum (March–June) is seen for slow-rise floods, which is associated with rain-on-snow
348 events that occur in the spring as precipitation falls as rain on melting snow (McCabe et al. 2007;
349 Ashley and Ashley 2008a). Hybrid floods display a maximum in May–July due to synoptic
350 rainfall and MCSs (Johnson and Schumacher 2006; Ashley and Ashley 2008a; Kunkel et al.
351 2012). The consistency of the seasonal distribution of floods with the literature, particularly the
352 agreement between flash flood seasonality with previous climatologies, provides confidence in
353 the flood-producing storm climatology developed herein.
354 The reason for the varying seasonality of different flood types is generally linked to
355 different underlying causes. Post-2006, the NCEI Storm Events database attributed causes to
356 flood reports, as shown in Table 2. Note that the percentages are the percent of flood causes post-
357 2006 excluding missing data (thus adding up to ~100% for each flood type). The leading cause
358 for all floods is heavy rain, comprising 94.8% of flash floods, 74.5% of slow-rise floods, and
359 89.0% of hybrid floods. This result is not surprising, given that heavy rainfall is a necessary
360 ingredient for flooding (Doswell et al. 1996), though the nature of heavy rainfall likely differs
361 between flood types. The second largest contributing cause to each flood type is heavy rain over
362 a burn area for flash floods (2.2%), heavy rain-on-snowmelt for slow-rise floods (20.7%), and
363 heavy rain from a tropical system for hybrid floods (3.9%). The heavy rain on snowmelt supports

Accepted for publication in *Monthly Weather Review*. DOI 10.1175/MWR-D-19-0020.1.

364 the springtime maximum for slow-rise floods (Fig. 2), while the heavy rain from a tropical
365 system explains some of the summertime maximum in hybrid floods.

366 To extend the seasonal analysis of floods beyond Fig. 2, the spatial distribution of each
367 flood type is examined by season (Figs. 3–5). Events per state from the NCEI Storm Events
368 Database are summed over the 12-year period and normalized by state area, to account for
369 differing state sizes. Flash floods in the winter (Fig. 3a) are confined mostly to the Gulf Coast,
370 Southeast, Ohio River Valley, and California. This distribution is due to increased north and
371 northeast moisture transport from the Gulf of Mexico in the Southeast and Ohio River Valley
372 (Trenberth 1999), while the California maxima is attributed to atmospheric rivers (ARs) that
373 affect the West Coast during the winter (Dettinger et al. 2011; Young et al. 2017; Saharia et al.
374 2017a). Transitioning to spring (Fig. 3b), flash flood occurrence spreads northward and eastward,
375 covering much of the eastern U.S., as warm-season convection begins and synoptic systems
376 frequent this area (Maddox et al. 1979). By summer (Fig. 3c), flash floods are nearly ubiquitous
377 over the entire CONUS, highlighting the predominant role of warm-season convection in causing
378 flash floods, as shown in Fig. 2 and other studies (Maddox et al. 1979; Davis 2001; Schumacher
379 and Johnson 2006). This result is expected, as most of the country is generally warm enough to
380 support convection in the summer. The maximum in flash floods in the Midwest and Plains is
381 due to MCSs, which contribute 30–70% of warm season rainfall to these regions (Fritsch et al.
382 1996) and are frequently associated with flooding (Michaud et al. 2001; Schumacher and
383 Johnson 2006; Ashley and Ashley 2008a; Kunkel et al. 2012). During the summer, the North
384 American monsoon is also at its peak (Adams and Comrie 1997), which explains the flash flood
385 maximum in the Southwest seen in Fig. 3c and observed in other studies (Ashley and Ashley
386 2008a; Kunkel et al. 2012; Saharia et al. 2017b). By fall (Fig. 3d), flash floods transition to the

Accepted for publication in *Monthly Weather Review*. DOI 10.1175/MWR-D-19-0020.1.

South (similar to the winter), clustered in the Southeast, Gulf Coast, East, and Ohio River Valley. Remnants of the North American monsoon signal is seen by the maximum in the Southwest. These seasonality results are broadly consistent with heavy rainfall analyses over the CONUS (Maddox et al. 1979; Brooks and Stensrud 2000; Schumacher and Johnson 2006; Kunkel et al. 2012), and flood climatologies (Michaud et al. 2001; Ashley and Ashley 2008a; Smith and Smith 2015; Saharia et al. 2017a, b), with minor discrepancies attributed to different data utilized in the present study.

Slow-rise floods exhibit a noticeably different seasonality than flash floods (Fig. 4), likely owing to different underlying causes (Table 2). During the winter (Fig. 4a), slow-rise floods are clustered in the Northeast and Ohio River Valley, where heavy rainfall from fronts and extratropical cyclones frequently occur (Schumacher and Johnson 2006; Kunkel et al. 2012). A secondary wintertime maximum is observed on the West Coast, which is affected by flooding from ARs and extratropical cyclones (Dettinger 2011; Kunkel et al. 2012; Young et al. 2017; Saharia et al. 2017b), as well rain-on-snow events (McCabe et al. 2007; Ashley and Ashley 2008a). The West Coast AR signal fades slightly by springtime (Fig. 4b), while the North Central and Upper Midwest display maxima, due to the occurrence of rain-on-snow events during the spring, (Michaud et al. 2001; McCabe et al. 2007; Ashley and Ashely 2008a; Berghuijs et al. 2016; Villarini et al. 2016), consistent with Table 2 and Fig. 2. The Northeast maximum remains in the spring, as synoptic systems still frequent this area (Kunkel et al. 2012). By the summer (Fig. 4c), the distribution of slow-rise flood events is less straightforward. A maximum along the eastern U.S. coastline is due to tropical systems (Schumacher and Johnson 2006; Ashley and Ashley 2008a; Kunkel et al. 2012; Villarini et al. 2014), while maxima in the Upper Midwest and Ohio River Valley are the result of synoptic systems or long-lived MCSs

Accepted for publication in *Monthly Weather Review*. DOI 10.1175/MWR-D-19-0020.1.

(Schumacher et al. 2006; Ashley and Ashley 2008a; Kunkel et al. 2012). The less apparent slow-rise flooding in the Interior West is explained by rain-on-snow events in the Rocky Mountains, which occur later in the season due to a longer snowfall season than other areas (McCabe et al. 2007), and upslope convection (Ashley and Ashley 2008a). During the fall (Fig. 4d), the distribution of slow-rise floods is similar to winter, as ARs begin affecting the West Coast, and frontal systems, as well as tropical cyclones frequent the eastern U.S. (Schumacher and Johnson 2006; Ashley and Ashley 2008a; Kunkel et al. 2012).

Hybrid flood seasonality (Fig. 5) is less intuitive than slow-rise or flash floods, given that it has characteristics of both. Despite the lack of clarity of results, hybrid floods are nonetheless important to consider, as some high-impact floods, such as the Colorado flood of 2013 (Gochis et al. 2015), fall into this category. During the winter (Fig. 5a), hybrid floods occur from the Southeast to Ohio River Valley and Northeast, as well as the Southwest. This pattern appears to be more similar to the flash flood wintertime distribution (Fig. 3a; also consistent with Table 2) and is attributed to the same causes. The springtime pattern of hybrid floods (Fig. 5b) appears to be a blend between the flash and slow-rise distribution (Fig.3b and 4b), thus displaying influences of rain-on-snow floods in northern and mountainous regions, as well as the start of warm-season convection in the Midwest. Springtime West Coast maxima are attributed to late-season ARs (Dettinger et al. 2011; Young et al. 2017). Summertime hybrid floods also show similarities to flash and slow-rise floods, with some East Coast locations displaying maxima, as well as the Upper Midwest, and Plains. This suggests that synoptic events, MCSs, and TCs that have "flashier" elements than slow-rise floods account for this spatial distribution. By fall (Fig. 5d), hybrid floods occur most notably in the Mid-Atlantic and Ohio River Valley, highlighting the predominance of tropical cyclones (namely Hurricanes Irene (2011), Hanna (2008), Gustav

Accepted for publication in *Monthly Weather Review*. DOI 10.1175/MWR-D-19-0020.1.

and Ike (2008); NHC) and frontal influences (Ashley and Ashley 2008; Kunkel et al. 2012; Villarini et al. 2014).

The total flood events per state from Figs. 3–5 is shown in Fig. 6. Flash floods (Fig. 6a) occur mostly to the east of the Rockies, with a secondary maximum in the Southwest. This result is reflective of the warm season convective and Southwest monsoon signals from Fig. 3. Slow-rise floods (Fig. 6b) show more of a northern maximum compared to flash floods, with most events clustered in the Northeast, Ohio River Valley, Upper Midwest, and Pacific Northwest. The northern maximum appears to be a result of the winter and springtime rain-on-snow events, while the Pacific Northwest maximum is attributed to ARs (Fig. 4). The distribution of hybrid floods (Fig. 6c) is less straightforward, predominantly occurring in the Mid-Atlantic, Ohio River Valley, and Plains. This suggests that hybrid floods experience the same flood-producing storms as both flash and slow-rise floods, but are distinguished by longer durations than flash floods and more convective characteristics than slow-rise floods, as will be shown in the following section.

b. Rainfall characteristics of flood-producing storms

In addition to examining when and where floods occurred, it is important to consider the distribution of rainfall characteristics over the CONUS using Stage IV rainfall data, especially since rainfall characteristics are lacking in the NCEI Storm Events Database. The episode frequency, average rainfall accumulation, area, and duration per Stage IV grid cell (~4 km x 4 km) for 12 years over the CONUS for each flood type is shown in Figs. 7, 8, and 10. The qualitative distribution rather than the quantitative value is more important to focus on for these results to compare regions with differing flood rainfall characteristics.

Flash flood rainfall characteristics (Fig. 7) show that flash floods frequently occur in the Mississippi and Ohio River Valleys (Fig. 7a), where there is also the highest average rainfall accumulation (Fig. 7b), largest average area (Fig. 7c), and moderate durations (15–24 h; Fig. 7d).

Accepted for publication in *Monthly Weather Review*. DOI 10.1175/MWR-D-19-0020.1.

Given the proximity to major rivers such as the Mississippi and Ohio Rivers, along with persistent moisture source from the Gulf of Mexico, and frequent year-round convection (Schumacher and Johnson 2006; Fig. 3), this result is consistent with expectations and with previous work (Michaud et al. 2001; Saharia et al. 2017a). Missouri and Arkansas stand out as notable hotspots for flash flood frequency and rainfall accumulation, which is unsurprising, due to the number of devastating floods in this location associated with MCSs (Ashley and Ashely 2008a; Schumacher and Johnson 2008, 2009). Notice that a secondary maximum in flash flood rainfall characteristics occurs in the Southwest, where, despite flash floods being only moderately frequent (Fig. 7a) with low average rainfall accumulation (Fig. 7b) and a small average area (Fig. 7c), they are associated with long-lived storms (over 24 h; Fig. 7d). These long-lived storms occur in January and from July–October, during the monsoon (not shown), and could be due to terrain-enhanced and terrain-locked precipitation (Neiman et al. 2004), as well as repeated convective initiation over the terrain. Maddox et al. (1979) and Michaud et al. (2001) similarly found that Western flash flood events were less frequent and had lower rainfall amounts, but were shorter in duration, which is inconsistent with our results. Our results include all flash floods in the Southwest, whereas Maddox et al. (1979) only considered 31 floods in the western CONUS that fit pattern recognition of synoptic conditions causing floods, while Michaud et al. (2001) only considered small basin (< 200 km^2 in area) floods. Both Maddox et al. (1979) and Michaud et al. (2001) are thus more limited in scope, while results from this study characterize the full spectrum of flash floods, which likely explains the discrepancy of long duration events in the Southwest with previous studies (Maddox et al. 1979; Michaud et al. 2001).

Accepted for publication in *Monthly Weather Review*. DOI 10.1175/MWR-D-19-0020.1.

Similar to the distribution of storm reports (Fig. 4), maximum values in slow-rise flood rainfall characteristics (Fig. 8) display a northern shift compared to flash floods. Slow-rise floods in the Northeast, Ohio River Valley, and the Upper Midwest are the most frequent (Fig. 8a), have the highest average rainfall accumulation (Fig. 8b), and largest area (Fig. 8c), with variable durations from 50–250 h (Fig. 8d). These regions displayed year-round flooding (Fig. 4), due to frequent synoptic forcing and long-lived MCSs (Schumacher and Jonson 2006; Ashley and Ashley 2008a; Kunkel et al. 2012). While the duration of slow-rise floods is only moderate in the Northeast and Ohio River Valley (Fig. 8d), long-duration (> 250 hours) slow-rise floods occur in the Northern Great Plains and Mississippi River Valley. In the Northern Great Plains, slow-rise floods are somewhat infrequent, with moderate rainfall accumulation and area, occurring mostly in the spring and summer (Fig. 4). This pattern is due to MCSs (Schumacher and Johnson 2006) and rain-on-snow events, with the latter comprising 66% of long-duration (>250 h) slow-rise floods (Fig. 9a; Table 3). The long-duration and moderately large floods in the lower Mississippi River Valley are consistent with a maximum frequency of long-duration (i.e., 5 days) widespread heavy rainfall events in the Gulf of Mexico, which were caused by cool-season synoptic cyclones, tropical cyclones, and summertime convection in nine cases examined by Schumacher and Johnson (2009). Flood reports show that long-duration events in the lower Mississippi Valley are primarily due to cool-season heavy rainfall (Fig. 9b; Table 3), showing that cool-season synoptic cyclones explain these long durations. Finally, moderate duration (~100 hours) and high rainfall accumulation slow-rise floods also occur in the Pacific Northwest, due to ARs (Davis 2001; Kunkel et al. 2012; Saharia et al. 2017a;) and rain-on-snow events (McCabe et al. 2007).

Accepted for publication in *Monthly Weather Review*. DOI 10.1175/MWR-D-19-0020.1.

Hybrid floods display a maximum in rainfall characteristics in the Central U.S., Ohio River Valley, and Mid-Atlantic (Fig. 10), which is between the location of maximum slow-rise and flash flood rainfall characteristics. In the Central U.S., Ohio River Valley, and Mid-Atlantic, hybrid floods occur most frequently (Fig. 10a), have the highest average rainfall accumulation (Fig. 10b), are the largest (Fig. 10c), and have moderate durations (40–100 hours; Fig. 10d). These locations are also where hybrid floods were frequently observed by storm reports (Fig. 5) and are likely the result of long-lived convection, tropical cyclones (Fig. 5), and frontal passages (Ashley and Ashley 2008; Kunkel et al. 2012; Villarini et al. 2014). The longest duration hybrid floods (> 100 h) are observed in the Gulf Coast (Fig. 10d), which highlights slow-moving tropical systems (Ashley and Ashley 2008a; Villarini et al. 2014).

c. Comparison of rainfall characteristics in flood-producing storms

While the spatial patterns shown above suggest differences in rainfall characteristics of the different flood-producing storm types, a direct comparison most prominently exhibits these differences. The distribution of episode total rainfall accumulation (normalized by storm area; Fig. 11a), episode maximum rain rate (Fig. 11b), total episode duration (Fig. 11c), and episode flood area (Fig. 11d) are compared between flash, slow-rise, and hybrid flood-producing storms. The total rainfall accumulation normalized by storm area is used rather than area-averaged rainfall due to the varying storm sizes between the different flood types for a more accurate comparison. Flash flood-producing storms exhibit high maximum rain rates (mean of 58 mm h^{-1} and up to 300 mm h^{-1}; Fig. 11b), the shortest duration (< 150 h; Fig. 11c), and smallest area (Fig. 11d), which is consistent with the convective nature of flash flood-producing storms (Maddox et al. 1979; Doswell et al. 1996; Davis 2001). However, rainfall accumulations are only moderate (Fig. 11a), due to the transient nature of these flood-producing storms, and maximum rain rates

Accepted for publication in *Monthly Weather Review*. DOI 10.1175/MWR-D-19-0020.1.

that are lower than hybrid flood-producing storms (mean of 71 mm h^{-1}). Given that hybrid flood-producing storms are slightly biased towards being composed of flash floods (Section 2b), but with a much larger area (Fig. 11d) and longer duration (Fig. 11c) than flash flood-producing storms, this suggests more intense and organized storms. These characteristics of hybrid flood-producing storms result in the highest rainfall accumulation of any flood type (Fig. 11a), due to high rain rates sustained over a long duration and large area (Eqn. 1). This is despite slow-rise flood-producing storms having a longer duration (Fig. 11c) and similarly large area (Fig. 11d). However, slow-rise flood-producing storms have a lower maximum rain rate (mean of 50 mm h^{-1}), which explains the lower rainfall accumulations, consistent with expectations (Davis 2001).

Differences in flood-producing storm rainfall characteristics are also summarized in Fig. 12, where flood episode average rain rate is plotted as a function of duration, and the size of the scatter points represents the area of the flood episode. Fig. 12 visualizes Eqn.1, which is a simple relationship showing that high rainfall accumulation is governed by high average rain rates sustained over a long-duration (though flood-producing storms usually exhibit a dominance of either rainfall rate or duration; Doswell et al. 1996). Note that average rain rates are calculated over the entire flood duration and area, thus yielding different results (and lower rain rates) than Fig. 11b. This visual representation of Eqn. 1 (Fig. 12) thus provides insight into the dominance and importance of flood "ingredients" in the various flood-producing storm types.

From Fig. 12, it is observed that flash flood-producing storms are intense (> up to 10 mm h^{-1}), small to moderate in size, and short duration (< 100 h), while slow-rise flood-producing storms are low-intensity (< 6 mm h^{-1}), large, and long-lived (> 300 h) events. Hybrid flood-producing storms are large and low intensity (< 6 mm h^{-1}) like slow-rise flood-producing storms, but with durations between flash and slow-rise flood-producing storms (generally < 300 h, with a

Accepted for publication in *Monthly Weather Review*. DOI 10.1175/MWR-D-19-0020.1.

few outliers). Combining this result with Fig. 11, hybrid flood-producing storms have the highest rainfall accumulation because they have higher maximum rain rates than slow-rise floods that are sustained longer than flash flood-producing storms. This relationship for the different flood-producing storms types is consistent with Eqn. 1, thus providing confidence that this flood climatology is robust and accurately captures flood characteristics unique to each flood type. Such a physically realistic climatology of various flood-producing storm types over the CONUS offers insight into the specific regions at risk for different impacts posed by these floods and their unique characteristics.

4. Conclusions

A flood-producing storm climatology over the CONUS from 2002–2013 was created to investigate the location, seasonality, and rainfall characteristics of flash, slow-rise, and hybrid flood-producing storms. The NCEI Storm Events Database documented where and when these floods occurred and is merged with stream gauge-indicated floods from the Shen et al. (2017) database to provide a robust indication of a significant hydrologic response to a causative meteorological event. Stage IV data supplemented the storm reports by providing rainfall data for the identified flood-producing storm cases, allowing for examination of flood-producing storm total rainfall accumulation, area, and duration. The methodology employed in this study allowed for the development of a flood-producing storm climatology over the CONUS, which is unique relative to previous studies by linking the specific meteorological rainfall characteristics to verified flood episodes. Additionally, this research fills the need for a flood climatology that examines characteristics of a range of flood-producing storm types and not just flash floods, which have been explored extensively in the literature (Maddox et al. 1979; Brooks and Stensrud 2000; Saharia et al. 2017a).

Accepted for publication in *Monthly Weather Review*. DOI 10.1175/MWR-D-19-0020.1.

570 The flood-producing storm climatology developed in this study was demonstrated to be
571 robust, as shown by the unique seasonal, spatial, and rainfall characteristics for the different
572 flood-producing storm types that are physically consistent with Doswell et al. (1996) and results
573 from prior studies. Additionally, this study provides a novel perspective on floods by analyzing
574 the detailed rainfall characteristics of numerous flood-producing storms over the CONUS. The
575 results for each flood-producing storm type are summarized as follows:

576 • Flash flood-producing storms
577 o Intense, short-duration, small to moderate-sized systems with low rainfall
578 accumulation
579 o Summertime maximum (due mostly to warm season convection)
580 o Occur most often east of the Rocky Mountains
581 o Most frequent, highest rainfall accumulation, largest area, and moderate duration
582 in Mississippi and Ohio River Valleys
583 o Moderate frequency, rainfall accumulation, and area, but longest duration in the
584 Southwest due to the monsoon
585 • Slow-rise flood-producing storms
586 o Low intensity, long-duration, large systems with low rainfall accumulations
587 o Spring–early summer maximum
588 o Occur most often in the Northeast, Ohio River Valley, Northern Plains, and
589 Pacific Northwest
590 o Due mostly to MCSs, synoptic events (including ARs), and rain-on-snowmelt
591 o Most frequent, highest rainfall accumulation, and largest area in the Northeast,
592 Ohio River Valley, and Upper Midwest

Accepted for publication in *Monthly Weather Review*. DOI 10.1175/MWR-D-19-0020.1.

- Moderate duration and frequency, but high rainfall accumulation in the Pacific Northwest due to ARs

- Hybrid flood-producing storms
  - Moderate intensity and duration, large systems, with high rainfall accumulations
  - Late spring–early summer maximum
  - Occur most often in the Central U.S. and Northeast
  - Due mostly to heavy rain and tropical systems
  - Most frequent, highest rainfall accumulation, largest area, and moderate duration in the Central U.S, Northeast, and Mid-Atlantic

While more detailed mesoscale and synoptic processes giving rise to the unique characteristics observed in each flood-producing storm type is beyond the scope of the current study, it is reasonable to conclude that these processes differ between flood types, as suggested by Doswell et al. (1996), Davis (2001), and observed in case-studies in the literature. Such cases include a flash flood from 6–7 May 2000 in eastern Missouri that was produced by a quasi-stationary MCS (Schumacher and Johnson 2008), multi-day AR flooding on the West Coast in December 2010 (Ralph and Dettinger 2012) characteristic of slow-rise flood-producing storms, and hybrid flood-producing storms in Colorado characterized by stratiform rainfall with embedded convection due to persistent upslope flow of moist neutral air (Gochis et al. 2015). Given the consistency of characteristics observed in flood-producing storms from this study with previous work, the mesoscale and synoptic dynamics unique to the aforementioned floods likely explain some of the observed differences among flood types in this climatology. It is important to study the full-spectrum of flood types, as was done in this study, given the range of behaviors exhibited in the different flood-producing storm types. The nature of this flood-producing storm

Accepted for publication in *Monthly Weather Review*. DOI 10.1175/MWR-D-19-0020.1.

climatology provides the potential to be useful for research and operational applications, especially considering the unique impacts that might result from different flood-producing storm types. An extensive documentation of where, when, how often, and how much rainfall occurred from different flood-producing storm types is valuable information for emergency mangers, city planners, and policy makers seeking efforts to protect their communities against flood-related risks.

Furthermore, the characteristics of these flood-producing storms provide a baseline for understanding the nature of these storms in a current climate so that potential future changes associated with a warming climate can be more accurately assessed. One application of this in future work is the utilization of high-resolution, convection-permitting simulations over the CONUS from 2002–2013 of the current and future climate (Liu et al. 2016) to examine potential changes to high-impact flood-producing storms from this climatology. This planned future work is similar to the Gutmann et al. (2018) study of hurricanes in a current and future climate, who finds higher precipitation rates in future hurricanes, providing further motivation for studying flood-producing storms in a future climate. These simulations will allow for an understanding of how the physical processes, in addition to the observed characteristics, of flood-producing storms in a future climate might change. Thus, this flood-producing storm climatology is one step toward a better understanding of the complex water, weather, and energy relationships in a current and future climate that can help inform the use of water-resources and risk posed by these disasters over the CONUS.

Acknowledgements

Accepted for publication in *Monthly Weather Review*. DOI 10.1175/MWR-D-19-0020.1.

The authors thank two anonymous reviewers and Steven Nelson for their comments and suggestions, which greatly improved the manuscript. This work is supported by the Colorado State University Water Center grant #1301164.

Accepted for publication in *Monthly Weather Review*. DOI 10.1175/MWR-D-19-0020.1.

References

Adams, D.K. and A. C. Comrie, 1997: The North American monsoon. *Bull. Amer. Meteor. Soc.*, **78**, 2197–2213.

Allen, M.R., and W.J. Ingram, 2002: Constraints on future changes in climate and the hydrologic cycle, *Nature*, **419**, 224–233.

Ashley, S.T., and W.S. Ashely, 2008a: The storm morphology of deadly flooding events in the United States. *Int. J. Climatol*, **28**, 493–503, https://doi.org/10.1002/joc.1554.

——, and ——, 2008b: Flood fatalities in the United States. *J. Appl. Meteor Climatol.*, **47**, 805 818, https://doi.org/10.1175/2007JAMC1611.1.

Barthold, F. E., T. E. Workoff, B. A. Cosgrove, J. J. Gourley, D. R. Novak, and K. M. Mahoney, 2015: Improving flash flood forecasts. *Bull. Amer. Meteor. Soc.*, **96**, 1859–1866, https://doi.org/10.1175/BAMS-D-14-00201.1.

Berghuijs, W. R., R.A. Woods, C. J. Hutton, and M. Sivapalan, 2016: Dominant flood generating mechanisms across the United States. *Geophysical Research Letters*, **43**, 4382–4390, https://doi.org/10.1002/2016GL068070.

Brooks, H.E., and D.J. Stensrud, 2000: Climatology of heavy rain events in the United States from hourly precipitation observations. *Mo. Wea. Rev*, **128**, 1194–1201.

Caracena, F. C., R. A. Maddox, L. R. Hoxit, and C. F. Chappell, 1979: Mesoanalysis of the Big Thompson storm. *Mo. Wea. Rev.*, **107**, 1–17.

Davis, R.S., 2001: Flash flood forecast and detection methods. *Severe Convective Storms, Meteor. Monogr.*, **No. 50**, Amer. Meteor. Soc., 481–525.

Dettinger, M.D., F. M. Ralph, T. Das, P. J. Neiman, and D. R. Cayan, 2011: Atmospheric Rivers,

Accepted for publication in *Monthly Weather Review*. DOI 10.1175/MWR-D-19-0020.1.

floods and the water resources of California. *Water*, **3**, 445–478. https://doi.org/10.3390/w3020445.

Doswell, C. A. III, H. E. Brooks, and R.A. Maddox, 1996: Flash flood forecasting: an ingredients-based methodology. *Wea. Forecasting*, **11**, 560–581.

Ferguson, A.P., and W. S. Ashley, 2017: Spatiotemporal analysis of residential flood exposure in the Atlanta, Georgia metropolitan area. *Nat. Hazards*, **87**, 989–1016, https://doi.org/10.1007/s11069-017-2806-6.

Freeman, A. and W. S. Ashley, 2017: Changes in the US hurricane disaster landscape: the relationship between risk and exposure. *Nat. Hazards*, **88**, 659–682, https://doi.org/10.1007/s11069-017-2885-4.

Fritsch, J.M., R. J. Kane, and C. R. Chelius,1996: The contribution of mesoscale convective weather systems to the warm-season precipitation in the United States. *Journal of Climate and Applied Meteorology*, **25**, 1333–1345.

Funk, W.T., 1991: Forecasting techniques utilized by the forecast branch of the National Meteorological Center during a major convective rainfall event. *Wea. Forecasting*, **6**, 584–564.

Gochis, D., and Coauthors, 2015: The great Colorado flood of September 2013. *Bull. Amer. Meteor. Soc.*, **96**, 1461–1487, https://doi.org/10.1175/BAMS-D-13-00241.1.

Gourley, J.J. and Coauthors, 2013: A unified flash flood database across the United States. *Bull. Amer. Meteor. Soc.*, **94**, 799–805, https://doi.org/10.1175/BAMS-D-12-00198.1.

Gutmann, E.D., and Coauthors, 2018: Changes in hurricanes from a 13-yr convection-permitting

Accepted for publication in *Monthly Weather Review*. DOI 10.1175/MWR-D-19-0020.1.

pseudo global warming simulation. *J. Climate*, **31**, 3643–3657, https://doi.org/10.1175/JCLI-D17-0391.1.

Herman, G.R. and R. S. Schumacher, 2018: Money doesn't grow on trees, but forecasts do: forecasting extreme precipitation with random forests. *Mon. Wea. Rev*., **146**, 1571–1600, https://doi.org/10.1175/MWR-D-17-0250.1.

Houze, R. A., K.L. Rasmussen, S. Medina, S.R. Brodzik, and U. Romatschke, 2011: Anomalous atmospheric events leading to the summer 2010 floods in Pakistan. *Bull. Amer. Meteor. Soc.*, **92**, 291–298, https://doi.org/10.1175/2010BAMS3173.1.

——, L.A. McMurdie, K.L. Rasmussen, A. Kumar, and M. M. Chaplin, 2017: Multiscale aspects of the storm producing the June 2013 flooding in Uttarakhand, India. *Mo. Wea. Rev*, **145**, 4447–4466, https://doi.org/10.1175/MWR-D-17-0004.1.

IPCC, 2013: Near-term climate change: projections and predictability. *In: Climate Change 2013: The Physical Science Basis. Contribution of Working Group I to the Fifth Assessment Report of the Intergovernmental Panel on Climate Change* [Stocker, T.F., D. Qin, G.-K. Plattner, M. Tignor, S.K. Allen, J. Boschung, A. Nauels, Y. Xia, V. Bex and P.M. Midgley (eds.)]. Cambridge University Press, Cambridge, United Kingdom and New York, NY, USA.

Kunkel, K.E, D. R. Easterling, D.A.R. Kristovich, B. Gleason, L. Stoecker, and R. Smith, 2012: Meteorological causes of the secular variations in observed extreme precipitation events for the conterminous United States. *J. Hydrometeor*., **13**, 1131–1141, https://doi.org/10.1175/JHM-D-11-0108.1.

Accepted for publication in *Monthly Weather Review*. DOI 10.1175/MWR-D-19-0020.1.

725 Lin Y., and K. E. Mitchell, 2005: The NCEP Stage II/IV hourly precipitation analyses:
726 Development and applications. *19th Conf. on Hydrology*, San Diego, CA, Amer. Meteor.
727 Soc., 1.2., [Available online at
728 https://ams.confex.com/ams/Annual2005/techprogram/paper_83847.htm.

729 Liu, C., and Coauthors, 2016: Continental-scale convection-permitting modeling of the current
730 and future climate of North America. *Clim Dyn*, **49**, 71–95,
731 https://doi.org/10.1007/s00382-016-3327-9.
732 Maddox, R. A., L. R. Hoxit, C. F. Chappell, and F. Caracena, 1978: Comparison of
733 Meteorological Aspects of the Big Thompson and City Flash Floods. *Mo. Wea. Rev*, **106**,
734 375–389.
735 ——, C.F. Chappell, and L. R. Hoxit, 1979: Synoptic and meso-α scale aspects of flash flood
736 events. *Bull. Amer. Meteor. Soc*., **60**, 115–123.
737 McCabe, G.J., M. P. Clark, and L. E. Hay, 2007: Rain-on-snow events in the Western United
738 States. *Bull. Amer. Meteor. Soc*., **March 2007**, 319–328.
739 Mei, Y. and E. N. Anagnostou, 2015: A hydrograph separation method based on information
740 from rainfall and runoff records. *Journal of Hydrology*, **523**, 636–649,
741 http://dx.doi.org/10.1016/j.jhydrol.2015.01.083.

742 Michaud, J.D., K. K. Hirschboeck, M. Winchell, 2001: Regional variations in small-basin floods
743 in the United States. *Water Resources Research*, **37**, 1405–1416.
744 Neilsen, E.R., G. R. Herman, R. C. Tournay, J. M. Peters, and R. S. Schumacher, 2015: Double
745 impact: when both tornadoes and flash floods threaten the same place at the same time.
746 *Wea. Forecasting*, **30**, 1673–1693, https://doi.org/10.1175/WAF-D-15-0084.1.

Accepted for publication in *Monthly Weather Review*. DOI 10.1175/MWR-D-19-0020.1.

747 Neiman, P.J., P. O. G. Persson, F. M. Ralph, D. P. Jorgensen, A. B. White, and D. E. Kingsmill,
748 2004: Modification of fronts and precipitation by coastal blocking during an intense
749 landfalling winter storm in Southern California: Observations during CALJET. *Mo. Wea.*
750 *Rev*, **132**, 242–273.

751 Nelson, B., O. P. Prat, D.-J. Seo, E. Habib, 2016: Assessment and implications of NCEP Stage
752 IV quantitative precipitation estimates for product intercomparisons. *Wea. Forecasting*,
753 **31**, 371–394, https://doi.org/10.1175/WAF-D-14-00112.1.

754 NHC, 2018: National Hurricane Center Tropical Cyclone Report: Hurricane Harvey:
755 https://www.nhc.noaa.gov/data/tcr/AL092017_Harvey.pdf .
756 NWS, 2007: National Weather Service instruction 10-1605: Storm data preparation.
757 Prein, A. F., C. Liu, K. Ikeda, S. B. Trier, R. M. Rasmussen, G. J. Holland, and M. Clark, 2017:
758 Increased rainfall volume from future convective storms in the US. *Nature Climate*
759 *Change*, **7**, 880–884, https://doi.org/10.1038/s41558-017-0007-7.

760 Qiang, Y., N. S. N. Lam, H. Cai, and L. Zou, 2017: Changes in exposure to flood hazards in
761 the United States. *Annals of the American Geographers*, **107**, 1332–1350,
762 https://doi.org/10.1080/24694452.2017.1320214 .

763 Ralph, F.M., and M.D. Dettinger, 2012: Historical and national perspectives on extreme West
764 Coast precipitation associated with atmospheric rivers during December 2010. *Bull.*
765 *Amer. Meteor. Soc.*, **93**, 783–790, https://doi.org/10.1175/BAMS-D-11-00188.1 .
766 Rasmussen, K. L. and R. A. Houze Jr., 2012: A flash-flooding storm at the steep edge of high
767 terrain: disaster in the Himalayas. *Bull. Amer. Meteor. Soc.*, **93**, 1713–1724.
768 https://doi.org/10.1175/BAMS-D-11-00236.1.

Accepted for publication in *Monthly Weather Review*. DOI 10.1175/MWR-D-19-0020.1.

769 ——., M. M. Chaplin, M.D. Zuluaga, and R.A. Houze Jr., 2016: Contribution of extreme
770 convective storms to rainfall in South America. *J. Hydrometeor*., **17**, 353–367**.**
771 Saharia, M., P. Kirsteetter, H. Vergara, J. J. Gourley, Y. Hong, and M. Giroud, 2017a: Mapping
772 flash flood severity in the United States. *J. Hydrometeor*., **18**, 397–411,
773 https://doi.org/10.1175/JHM-D-16-0082.1.

774 ——, ——, ——, ——, and ——, 2017b: Characterization of floods in the United States. *Journal of*
775 *Hydrology*, **548,** 524–535, http://dx.doi.org/10.1016/j.jhydrol.2017.03.010.

776 Schroeder, A.J., and Coauthors, 2016a: The development of a flash flood severity index.
777 *Journal of Hydrology*, **541**, 523–532, http://dx.doi.org/10.1016/j.jhydrol.2016.04.005 .

778 ——, J. Basara, J. M. Sheperd, S. Nelson, 2016b: Insights into atmospheric contributors to
779 urban flash flooding across the United States using an analysis of rawinsode data and
780 associated calculated parameters. *J. Appl. Meteor. Climatol.*, **55**, *313–323*,
781 https://doi.org/10.1175/JAMC-D-14-0232.1.

782 Schumacher, R. S., and R. H. Johnson, 2006: Characteristics of U.S. extreme rain events during
783 1999–2003. *Wea. Forecasting*, **21**, 69–85.
784 ——, and ——, 2008: Mesoscale processes contributing to extreme rainfall in a midlatitude warm
785 season flash flood. *Mon. Wea. Rev.*, **136**, 3964–3986,
786 https://doi.org/10.1175/2008MWR2471.1.

787 ——, and ——, 2009a: Quasi-stationary, extreme-rain-producing convective systems associated
788 with midlevel cyclonic circulations. *Wea. Forecasting*, **42**, 555–574,
789 https://doi.org/10.1175/2008WAF2222173.1.

Accepted for publication in *Monthly Weather Review*. DOI 10.1175/MWR-D-19-0020.1.

790 Shen, S., Y. Mei, and E. M. Anagnostou, 2017: A comprehensive database of flood events in the
791 contiguous United States from 2002 to 2013. *Bull. Amer. Meteor. Soc.*, **98**, 1493–1502.
792 https://doi.org/10.1175/BAMS-D-16-0125.1.

793 Smith, B.K. and J.A. Smith, 2015: The flashiest watersheds in the contiguous United States. *J.*
794 *Hydrometeor*., **16**, 2365–2381, https://doi.org/10.1175/JHM-D-14-0217.1.

795 Stevenson, S. N., and R.S. Schumacher, 2014: A 10-year survey of extreme rainfall events in the
796 central and eastern United States using gridded multisensor precipitation analyses. *Mon.*
797 *Wea. Rev*., **142**, 3147–3162, https://doi.org/10.1175/MWR-D-13-00345.1.

798 Trenberth, K.E., 1999: Conceptual framework for changes of extremes of the hydrological cycle
799 with climate change. *Climate Change*, **42**, 327–339.
800 Villarini, G., R. Goska, J. A. Smith, and G. A. Vecchi, 2014: North Atlantic tropical cyclones
801 and U.S. flooding. *Bull. Amer. Meteor. Soc*., **95**, 1381–1388,
802 https://doi.org/10.1175/BAMS-D-13-00060.1 .

803 ——, 2016: On the seasonality of flooding across the continental United States. *Advances in*
804 *Water Resources*, **87**, 80–91, http://dx.doi.org/10.1016/j.advwatres.2015.11.009.

805 Wing, O. E. J., P.D. Bates, A. M. Smith, C. C. Sampson, K. A. Johnson, J. Fargione, and P.
806 Morefield, 2018: Estimates of present and future flood risk in the conterminous United
807 States. *Environ. Res. Lett*., **13**, 1–7, https://doi.org/10.1088/1748-9326/aaac65.

808 Young, A. M., K. T. Skelly, and J. M. Cordeira, 2017: High-impact hydrologic events and
809 atmospheric rivers in California: An investigation using the NCEI Storm Events
810 Database. *Geophysical Research Letters*, **44**, 3393–3401,

Accepted for publication in *Monthly Weather Review*. DOI 10.1175/MWR-D-19-0020.1.

https://doi.org/10.1002/2017GL073077.

Accepted for publication in *Monthly Weather Review*. DOI 10.1175/MWR-D-19-0020.1.

Tables

Table 1. The number of flash, slow-rise, and hybrid flood-producing storms for events (episodes) in the NCEI Storm Event Database in the left (right) column that match flooded stream gauge locations from the Shen et al. (2017) database. The row labeled "all" is the sum of flood episodes for all flood types.

	Events	**Episodes**
Flash floods	15,932	2,808
Slow-rise floods	10,614	1,638
Hybrid floods	11,120	1,113
All	37,666	5,559

Table 2. Percentage of flood causes comprising each type of flood, where bolded values indicate the largest percentage and bolded-italicized values indicate the second largest percentage. Flood causes only include post-2006 NCEI Storm Events data and exclude missing data from the calculation.

Flood type	Dam/ levee break	Heavy rain	Heavy rain/ burn area	Heavy rain/ snowmelt	Heavy rain/ tropical system	Ice jam	Planned dam release
Flash	0.7	**94.8**	***2.2***	0.5	1.7	0.1	0.1
Slow rise	0.4	**74.5**	0.3	***20.7***	2.4	2.4	0.3
Hybrid	3.2	**89.0**	0.3	2.5	***3.9***	0.4	0.7

Accepted for publication in *Monthly Weather Review*. DOI 10.1175/MWR-D-19-0020.1.

Table 3. Seasonality of long-duration (> 250 h) slow-rise flood causes in the Northern Great Plains and Lower Mississippi Valley for causes that comprise over 25% of the total. The peak season for each flood cause in each region is bolded.

Northern Great Plains	Fall	Winter	Spring	Summer	Total
Heavy rain	2%	0%	4%	**24%**	30%
Heavy rain/ snowmelt	0%	0%	**45%**	21%	66%
Lower Mississippi Valley					
Heavy rain	17%	17%	**48%**	4%	86%

Accepted for publication in *Monthly Weather Review*. DOI 10.1175/MWR-D-19-0020.1.

Figure Captions

FIG 1. An example of the methodology used to identify flood-producing storm rainfall from Stage IV rainfall data. A flash flood in Virginia occurred from 0300–1600 UTC on 7 October 2006, with its flood centroid shown by the star, flooded stream gauges from the Shen et al. (2017) database in red dots, and largest contiguous area of Stage IV accumulated precipitation (shaded; mm) over the 75th percentile outlined in black, as identified from an object-identifier tool in Python.

FIG 2. Number of flood episodes per month summed from 2002–2013, where cyan represents flash floods, dark blue represents hybrid, and grey represents slow-rise floods.

FIG 3. Number of flash flood events per state (fill; normalized by state area) and locations of USGS gauge-indicated floods from the Shen et al. (2017) database (black dots) over the CONUS from 2002–2013 for a) winter (DJF), b) spring (MAM), c) summer (JJA), and d) fall (SON).

FIG 4. As in Fig. 3, but for slow-rise floods.

FIG 5. As in Fig. 3, but for hybrid floods.

FIG 6. Number of a) flash, b) slow-rise, and c) hybrid flood events per state (fill; normalized by state area) and locations of USGS gauge-indicated floods from the Shen et al. (2017) database (black dots) over the CONUS from 2002–2013.

FIG 7. Flash flood a) episode count, b) average rain accumulation, c) average area, and d) average duration (h) per Stage IV grid cell from 2002–2013. Values in a), b), and c) are in logarithmic scales, while those in b) and c) have been normalized by a scaling factor (number of flood events in Stage IV grid cell/total number of flood events).

FIG 8. As in Fig. 7, but for slow-rise floods

Accepted for publication in *Monthly Weather Review*. DOI 10.1175/MWR-D-19-0020.1.

FIG 9. Cause of long-duration (> 250 h) slow-rise floods in the a) Northern Great Plains (n=82) and b) Lower Mississippi Valley (n=23) from post-2006 NCEI Storm Events data. The size of different colors in the circle shows the percentage of each flood cause (green=heavy rain, blue=heavy rain on snowmelt, purple=ice jam, orange=dam release, and red=heavy rain over burn area).

FIG 10. As in Fig. 7, but for hybrid floods.

FIG 11. Boxplots of a) rainfall accumulation normalized by flood area (mm km^{-2}), b) maximum rain rate (mm h^{-1}), c) flood duration (h), and d) flood area (km^2) for flash (red box), slow-rise (cyan box), and hybrid flood episodes (purple box). Black dots indicate outliers.

FIG 12. Average rain rate (mm h^{-1}) as a function of the log of duration (h) for flash (red dots), slow-rise (blue dots), and hybrid (purple dots) floods, where the size of the dot represents the area of the flood.

Accepted for publication in *Monthly Weather Review*. DOI 10.1175/MWR-D-19-0020.1.

Figures

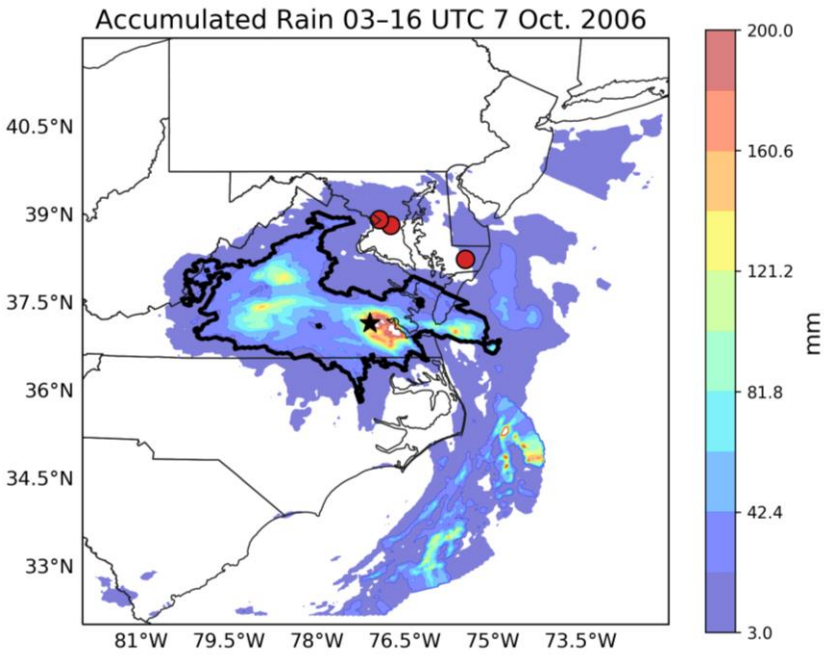

FIG 1. An example of the methodology used to identify flood-producing storm rainfall from Stage IV rainfall data. A flash flood in Virginia occurred from 0300–1600 UTC on 7 October 2006, with its flood centroid shown by the star, flooded stream gauges from the Shen et al. (2017) database in red dots, and largest contiguous area of Stage IV accumulated precipitation (shaded; mm) over the 75th percentile outlined in black, as identified from an object-identifier tool in Python.

Accepted for publication in *Monthly Weather Review*. DOI 10.1175/MWR-D-19-0020.1.

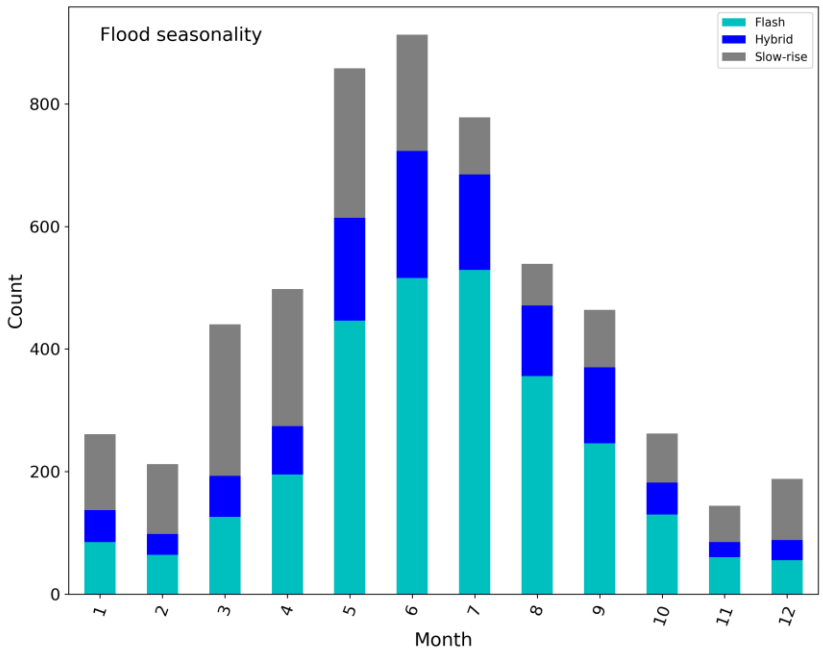

914

915 **FIG 2**. Number of flood episodes per month summed from 2002–2013, where cyan represents

916 flash floods, dark blue represents hybrid, and grey represents slow-rise floods.

917

918

919

920

921

922

923

924

925

926

927

Accepted for publication in *Monthly Weather Review*. DOI 10.1175/MWR-D-19-0020.1.

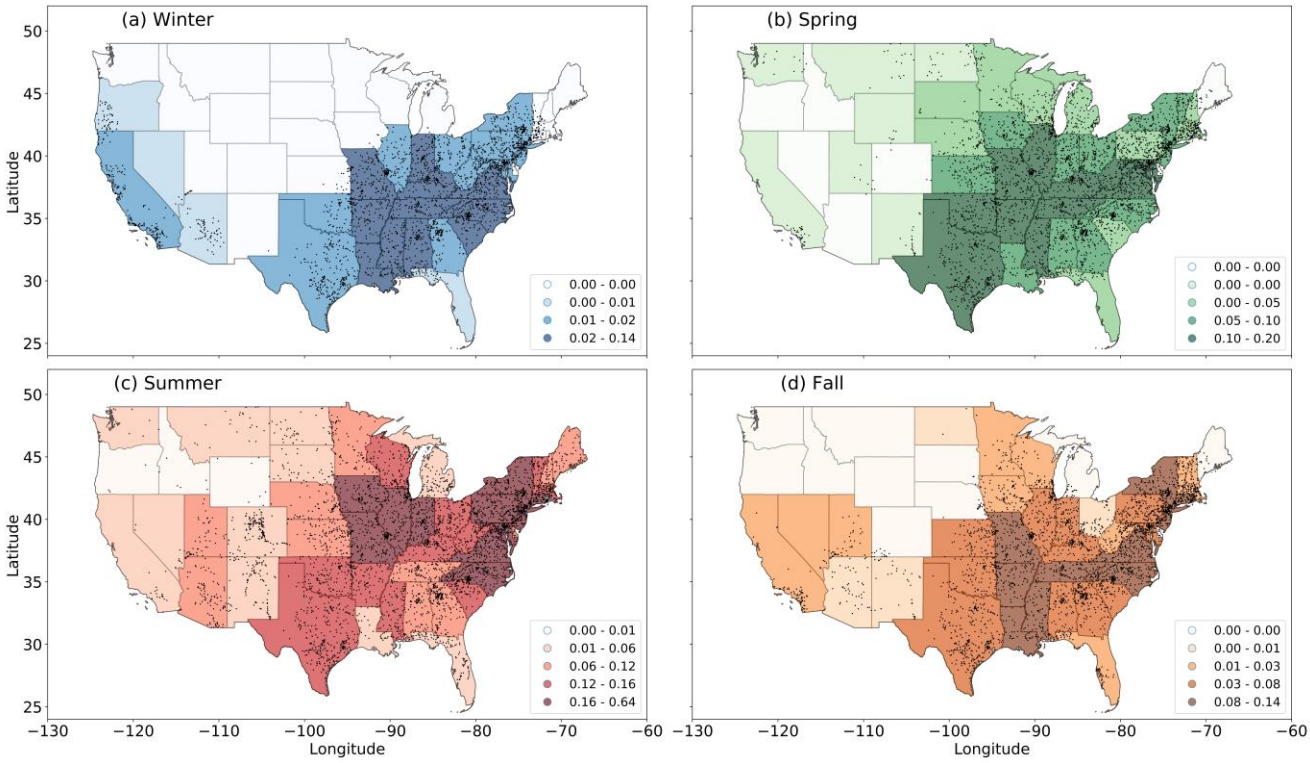

FIG 3. Number of flash flood events per state (fill; normalized by state area) and locations of USGS gauge-indicated floods from the Shen et al. (2017) database (black dots) over the CONUS from 2002–2013 for a) winter (DJF), b) spring (MAM), c) summer (JJA), and d) fall (SON).

Accepted for publication in *Monthly Weather Review*. DOI 10.1175/MWR-D-19-0020.1.

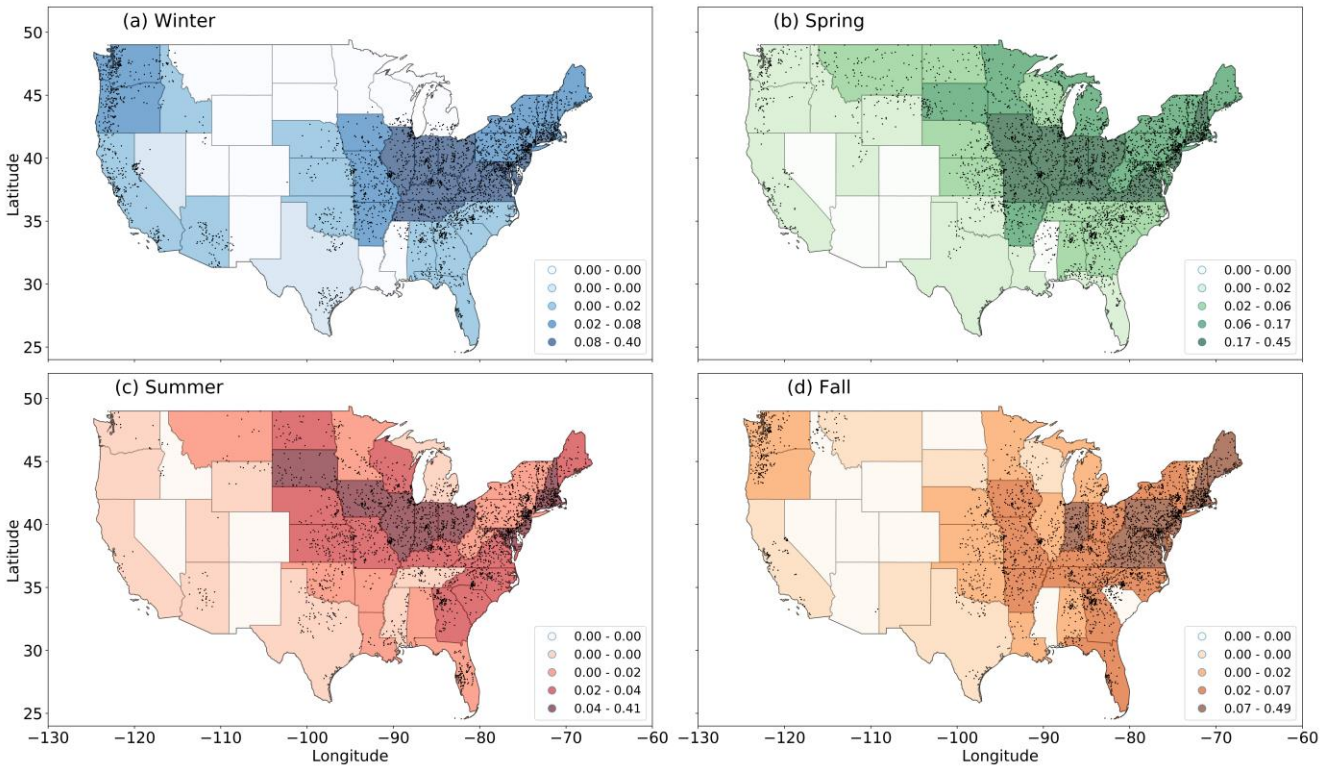

FIG 4. As in Fig. 3, but for slow-rise floods.

Accepted for publication in *Monthly Weather Review*. DOI 10.1175/MWR-D-19-0020.1.

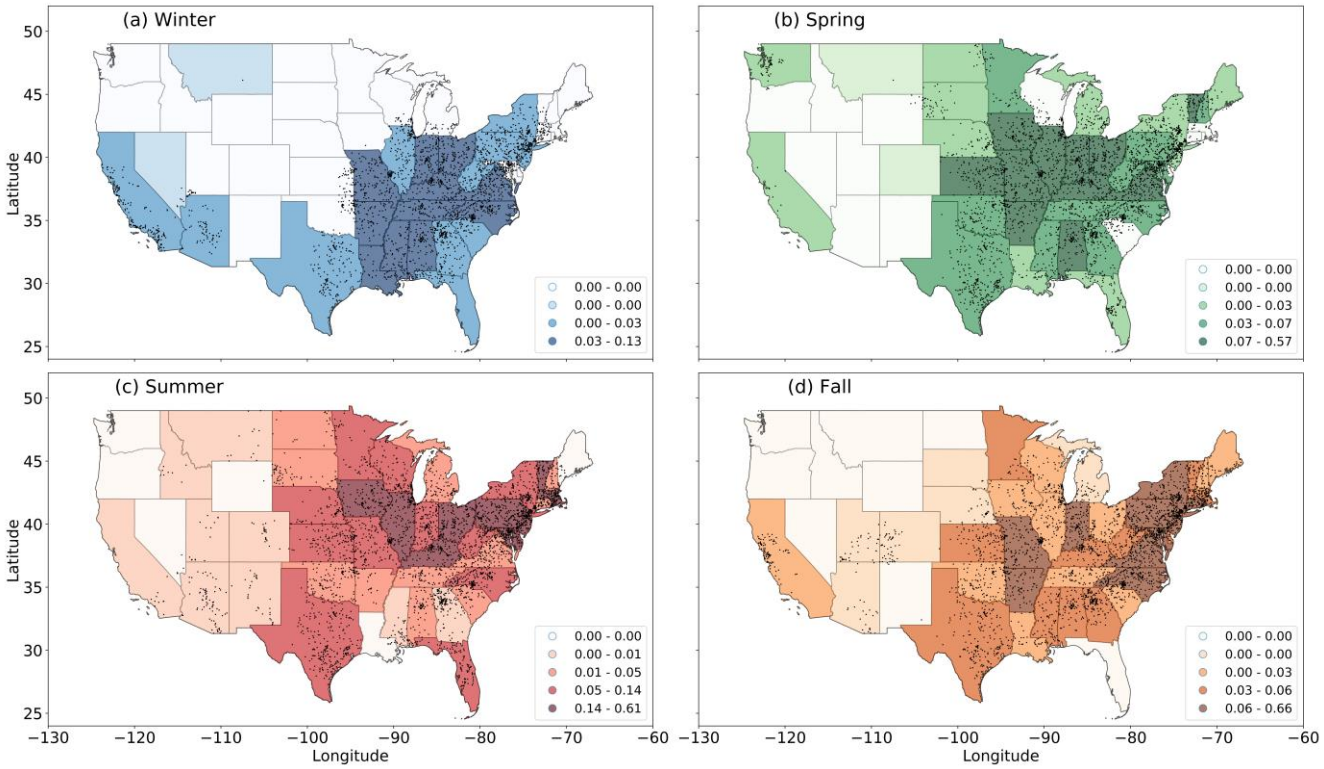

FIG 5. As in Fig. 3, but for hybrid floods.

Accepted for publication in *Monthly Weather Review*. DOI 10.1175/MWR-D-19-0020.1.

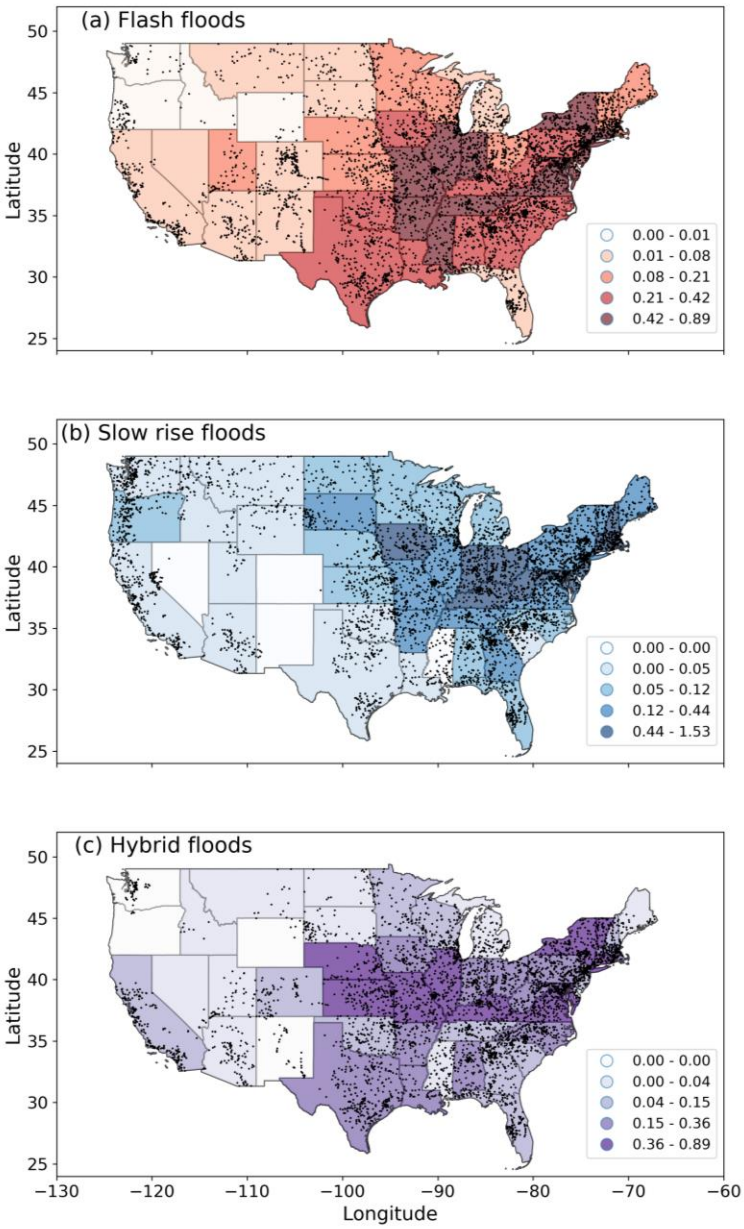

961

962 **FIG 6**. Number of a) flash, b) slow-rise, and c) hybrid flood events per state (fill; normalized by
963 state area) and locations of USGS gauge-indicated floods from the Shen et al. (2017) database
964 (black dots) over the CONUS from 2002–2013.

965

966

967

Accepted for publication in *Monthly Weather Review*. DOI 10.1175/MWR-D-19-0020.1.

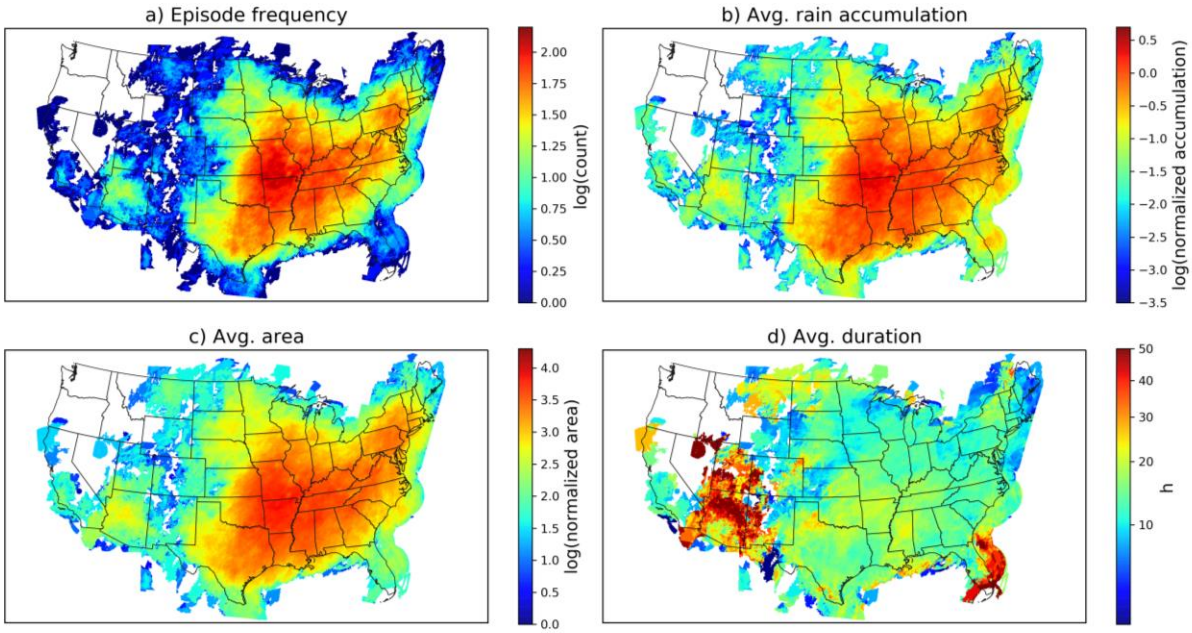

FIG 7. Flash flood a) episode count, b) average rain accumulation, c) average area, and d) average duration (h) per Stage IV grid cell from 2002–2013. Values in a), b), and c) are on logarithmic scales, while those in b) and c) have been normalized by a scaling factor (number of flood events in Stage IV grid cell/total number of flood events).

Accepted for publication in *Monthly Weather Review*. DOI 10.1175/MWR-D-19-0020.1.

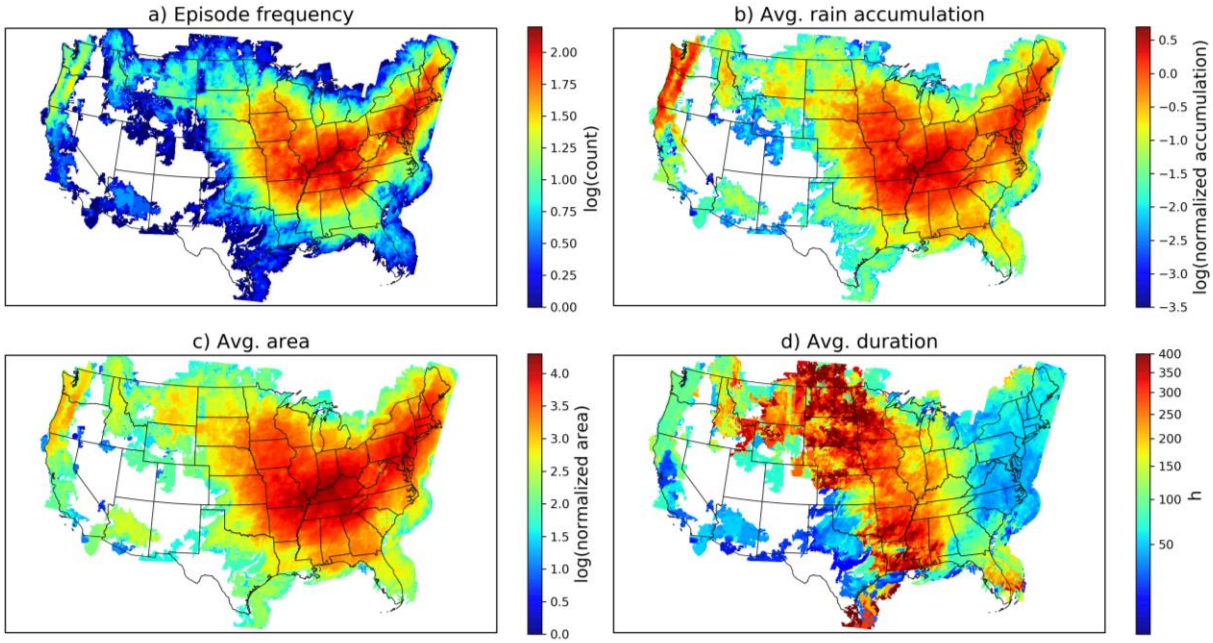

FIG 8. As in Fig. 7, but for slow-rise floods.

Accepted for publication in *Monthly Weather Review*. DOI 10.1175/MWR-D-19-0020.1.

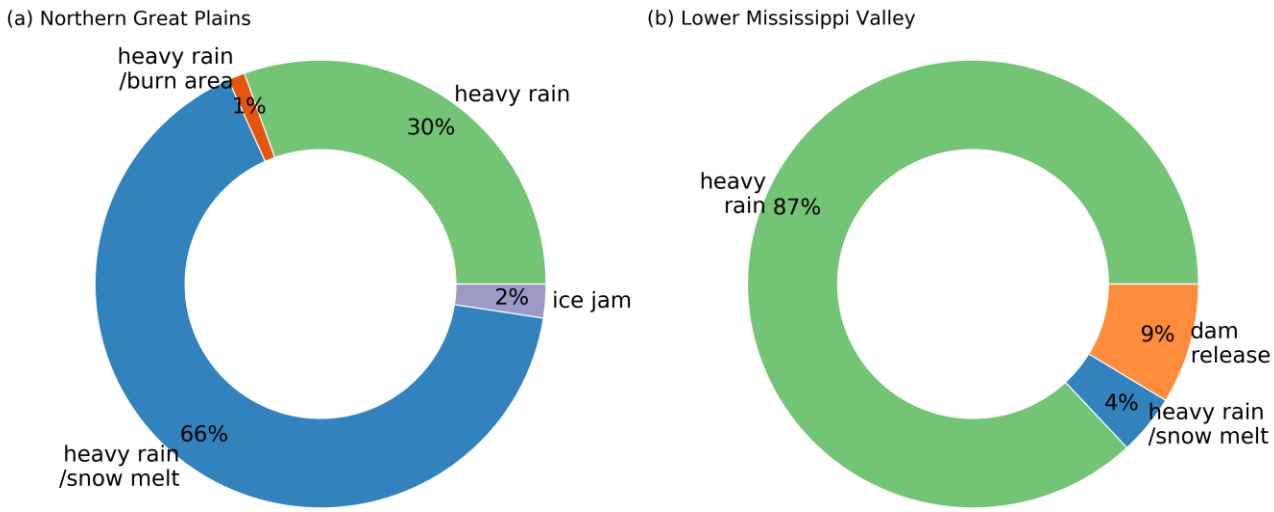

990

991 **FIG 9**. Cause of long-duration (> 250 h) slow-rise floods in the a) Northern Great Plains (n=82)
992 and b) Lower Mississippi Valley (n=23) from post-2006 NCEI Storm Events data. The size of
993 different colors in the circle shows the percentage of each flood cause (green=heavy rain,
994 blue=heavy rain on snowmelt, purple=ice jam, orange=dam release, and red=heavy rain over
995 burn area).

996

997

998

999

Accepted for publication in *Monthly Weather Review*. DOI 10.1175/MWR-D-19-0020.1.

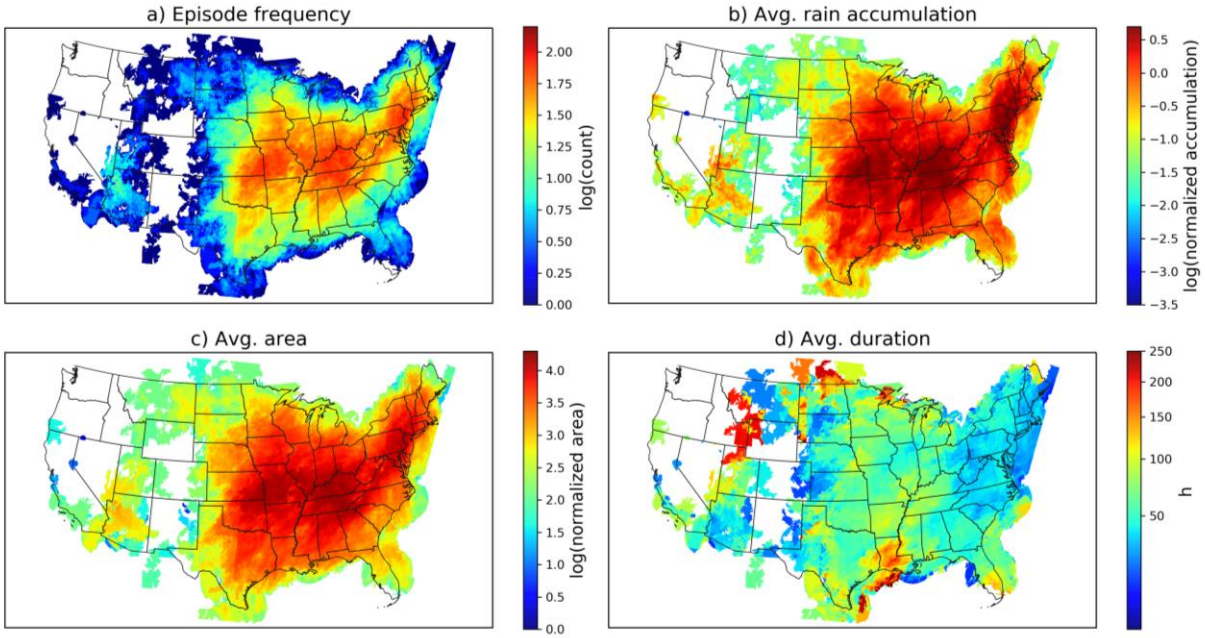

FIG 10. As in Fig. 7, but for hybrid floods.

Accepted for publication in *Monthly Weather Review*. DOI 10.1175/MWR-D-19-0020.1.

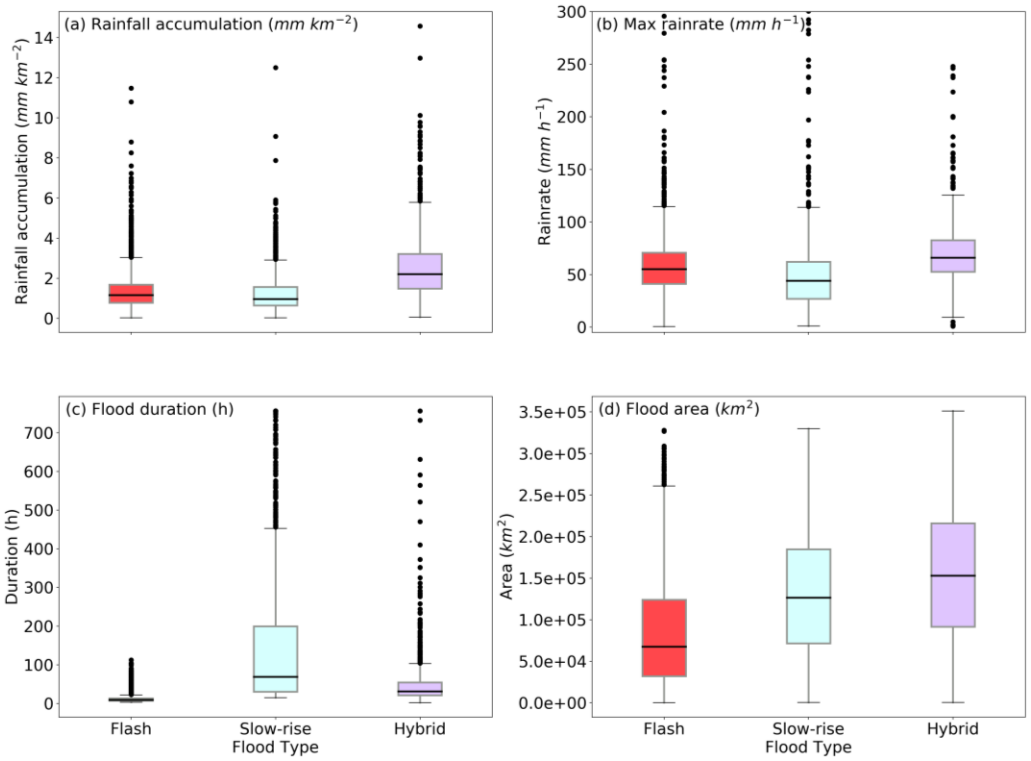

FIG 11. Boxplots of a) rainfall accumulation normalized by flood area (mm km^{-2}), b) maximum rain rate (mm h^{-1}), c) flood duration (h), and d) flood area (km^2) for flash (red box), slow-rise (cyan box), and hybrid flood episodes (purple box). Black dots indicate outliers.

Accepted for publication in *Monthly Weather Review*. DOI 10.1175/MWR-D-19-0020.1.

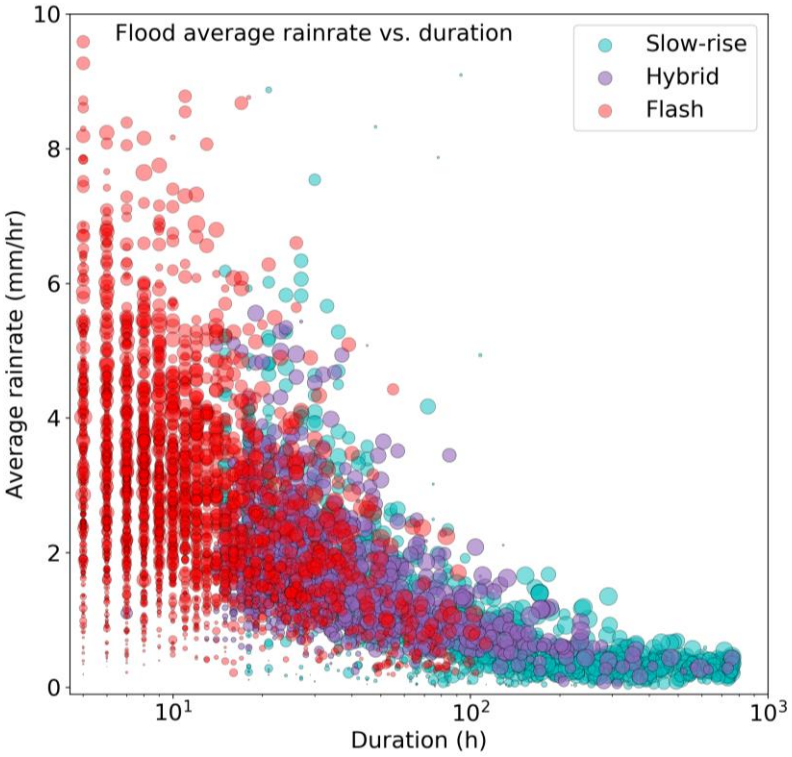

FIG 12. Average rain rate (mm h^{-1}) as a function of the log of duration (h) for flash (red dots), slow-rise (blue dots), and hybrid (purple dots) floods, where the size of the dot represents the area of the flood.

Accepted for publication in *Monthly Weather Review*. DOI 10.1175/MWR-D-19-0020.1.